LETTER

https://doi.org/10.1038/s41586-018-0588-y

The dispersion–brightness relation for fast radio bursts from a wide-field survey

R. M. Shannon[1,2,3,4]*, J.-P. Macquart[3,5]*, K. W. Bannister[4], R. D. Ekers[3,4], C. W. James[3,5], S. Osłowski[1], H. Qiu[4,5,6], M. Sammons[3], A. W. Hotan[7], M. A. Voronkov[4], R. J. Beresford[4], M. Brothers[4], A. J. Brown[4], J. D. Bunton[4], A. P. Chippendale[4], C. Haskins[7], M. Leach[4], M. Marquarding[4], D. McConnell[4], M. A. Pilawa[4], E. M. Sadler[5,6], E. R. Troup[4], J. Tuthill[4], M. T. Whiting[4], J. R. Allison[8], C. S. Anderson[7], M. E. Bell[4,5,9], J. D. Collier[4,10], G. Gürkan[7], G. Heald[7] & C. J. Riseley[7]

Despite considerable efforts over the past decade, only 34 fast radio bursts—intense bursts of radio emission from beyond our Galaxy—have been reported[1,2]. Attempts to understand the population as a whole have been hindered by the highly heterogeneous nature of the searches, which have been conducted with telescopes of different sensitivities, at a range of radio frequencies, and in environments corrupted by different levels of radio-frequency interference from human activity. Searches have been further complicated by uncertain burst positions and brightnesses—a consequence of the transient nature of the sources and the poor angular resolution of the detecting instruments. The discovery of repeating bursts from one source[3], and its subsequent localization[4] to a dwarf galaxy at a distance of 3.7 billion light years, confirmed that the population of fast radio bursts is located at cosmological distances. However, the nature of the emission remains elusive. Here we report a well controlled, wide-field radio survey for these bursts. We found 20, none of which repeated during follow-up observations between 185–1,097 hours after the initial detections. The sample includes both the nearest and the most energetic bursts detected so far. The survey demonstrates that there is a relationship between burst dispersion and brightness and that the high-fluence bursts are the nearby analogues of the more distant events found in higher-sensitivity, narrower-field surveys[5].

Since the beginning of 2017, we have been surveying for fast radio bursts (FRBs) using a subset of the Australian Square Kilometre Array Pathfinder[6] (ASKAP), a radio-telescope array comprising 36 antennas that is currently being commissioned. Each antenna is equipped with a phased-array-feed (PAF) receiver that is sensitive to 30 deg^2 on the sky at the prime focus of a 12-metre reflector. The searches, conducted at a central frequency of 1.3 GHz, have used a fly's-eye configuration, with each of 5−12 available antennas pointed towards a different area of sky, widening our field of view to target the brightest portion of the burst population. The system set-up and search algorithms are identical to those reported previously from ASKAP[7]. The PAFs allow full sampling of the focal plane, making it possible to measure the burst positions with as little as 10×10 arcmin uncertainty[7] (90% confidence), and the fluence of each burst to better than 20% accuracy[7]—in contrast with previous searches where burst positions were unconstrained within the antenna beam pattern, and burst fluences could be uncertain by factors greater 10. The searches have been conducted at 57 high Galactic latitude pointings, $|b| = 50 \pm 5$ deg, removing the need to account for potential bias in the latitude dependence of the rate[8] and minimizing the contribution of the Galaxy to the electron column density. Observations of these pointings were interleaved with short scans of known pulsars to check system performance (see Supplementary Information, section 1). Pointings were revisited a median of 570 times over the course of the survey. In total, our survey exposure is 5.1×10^5 deg^2 h (see Supplementary Information, section 1).

We have discovered 20 FRBs in total (including FRB 170107, reported previously[7]), the properties of which are listed in Table 1. The electron column densities towards the bursts, expressed as dispersion measures, range from 114 pc cm^{-3} to 992 pc cm^{-3}. The dispersion measures contain contributions from the Milky Way, the host galaxy, and the intergalactic medium. The Galactic dispersion-measure contributions are likely to be less than 60 pc cm^{-3} for all of our bursts. Assuming a negligible circumburst environment, the host galaxy is likely to have a similar median contribution[9] (see Supplementary Information, section 4). Larger contributions would be possible if the bursts were embedded in dense nebulae such as supernova remnants or in galaxy centres. However, our lowest dispersion-measure events show that for some objects this contribution does not exceed 50−120 pc cm^{-3}. We also assume that the intergalactic medium is uniformly distributed, and use a standard distance/dispersion-measure relationship[10] to infer distances from the extragalactic dispersion-measure component. For the nearest (and hence lowest dispersion measure) bursts, larger stochasticity in the intergalactic dispersion-measure contribution would be expected, as it will depend strongly on the host location within the corresponding local large-scale structure[11], which has a characteristic size scale of 30 Mpc. For more distant objects, bursts will propagate through many voids and walls in the large-scale structure and therefore will only have modest 10−20% scatter[11]. Our sample includes the lowest hitherto reported dispersion measure for a burst (FRB 171020), which has a column-density excess beyond the Milky Way[12] of 80 pc cm^{-3}. Given the assumed distance/dispersion-measure model described above, this burst would have originated at a distance of approximately 130 Mpc (at a redshift, z, of around 0.03). This burst has one of the poorest localizations (30×50 arcmin ellipse, 90% confidence) in our sample, because it was detected in a corner beam. However, there is only one galaxy catalogued at a distance of less than 210 Mpc (z less than 0.05) within the uncertainty region of the FRB. This is the distorted Sc-type spiral galaxy PGC 068417, at a distance of 37 Mpc[13] ($z = 0.0087$). A second galaxy at the edge of the error box, PGC 3094828, has a catalogued redshift of $z = 0.0665$, placing it at a distance of 275 Mpc (ref. [14]). Low-dispersion bursts such as FRB 171020 offer the potential for detailed host-galaxy studies.

The measured fluences range from 34 Jy ms to 420 Jy ms, with the latter being the highest well constrained fluence (see Supplementary Information, section 4). Above our completeness threshold of a signal-to-noise ratio of 9.5—which corresponds to a fluence of 26 Jy ms $(w/1.26\ \mathrm{ms})^{-1/2}$ for a pulse duration w matching our time resolution of 1.26 ms—the event rate is 37 ± 8 per day over the entire sky

[1]Centre for Astrophysics and Supercomputing, Swinburne University of Technology, Hawthorn, Victoria, Australia. [2]ARC Centre of Excellence for Gravitational Wave Discovery (OzGrav), Hawthorn, Australia. [3]International Centre for Radio Astronomy Research, Curtin Institute of Radio Astronomy, Curtin University, Perth, Western Australia, Australia. [4]CSIRO Astronomy and Space Science, Australia Telescope National Facility, Epping, New South Wales, Australia. [5]ARC Centre of Excellence for All-Sky Astrophysics (CAASTRO), Sydney, Australia. [6]Sydney Institute for Astronomy, School of Physics, University of Sydney, Sydney, New South Wales, Australia. [7]CSIRO Astronomy and Space Science, Australia Telescope National Facility, Bentley, Western Australia, Australia. [8]Sub-Department of Astrophysics, Department of Physics, University of Oxford, Oxford, UK. [9]School of Mathematics and Physical Sciences, University of Technology Sydney, Sydney, New South Wales, Australia. [10]School of Computing, Engineering, and Mathematics, Western Sydney University, Sydney, New South Wales, Australia. *e-mail: rshannon@swin.edu.au; J.Macquart@curtin.edu.au

Table 1 | Properties of ASKAP FRBs

FRB	Time (TAI*)	DM (pc cm^{-3})	E_ν (Jy ms)	R.A. (hh:mm)†	Dec. (dd:mm)†	g_l (deg.)	g_b (deg.)	w (ms)	S/N‡	T_{obs} (d)	$T_{\pm 15}$ (h)
170107	20:05:45.1393(1)	609.5(5)	58(3)	11:23.3(7)	−05:00(10)	266.0	54.1	2.4(2)	16.0	27.9	15
170416	23:11:49.7994(2)	523.2(2)	97(2)	22:13(1)	−55:02(9)	337.6	−50.0	5.0(6)	13.0	16.2	31
170428	18:03:11.7003(2)	991.7(9)	34(2)	21:47(2)	−41:51(20)	359.2	−49.9	4.4(5)	10.5	31.6	22
170707	06:18:11.3548(2)	235.2(6)	52(3)	02:59(2)	−57:16(20)	269.1	−50.5	3.5(5)	9.5	11.3	56
170712	13:22:54.39488(8)	312.79(7)	53(2)	22:36(1)	−60:57(10)	329.3	−51.6	1.4(3)	12.7	7.7	32
170906	13:07:33.48832(8)	390.3(4)	74(7)	21:59.8(4)	−19:57(10)	34.2	−49.5	2.5(3)	17.0	32.7	95
171003	04:08:00.78117(9)	463.2(1.2)	81(5)	12:29.5(7)	−14:07(20)	283.4	46.3	2.0(2)	13.8	27.3	67
171004	03:24:16.2501(1)	304.0(3)	44(2)	11:57.6(8)	−11:54(10)	282.2	48.9	2.0(3)	10.9	30.5	84
171019	13:27:17.09738(1)	460.8(1.1)	219(5)	22:17.5(5)	−08:40(7)	52.5	−49.3	5.4(3)	23.4	17.6	57
171020¶	10:28:35.59870(4)	114.1(2)	200^{+500}_{-100}	22:15(3)	−19:40(40)	29.3	−51.3	1.7(2)	19.5	32.7	95
171116	15:00:10.3052(2)	618.5(5)	63(2)	03:31.0(6)	−17:14(10)	205.0	−49.8	3.2(5)	11.8	45.7	102
171213	14:23:17.46705(3)	158.6(2)	133(12)	03:39(2)	−10:56(20)	200.6	−48.3	1.5(2)	25.1	35.5	118
171216	17:59:47.82229(9)	203.1(5)	40(2)	03:28(1)	−57:04(10)	273.9	−48.4	1.9(3)	8.0	7.7	26
180110‖	07:35:11.9590(1)	715.7(2)	420(20)	21:53.0(7)	−35:27(7)	7.8	−51.9	3.2(2)	35.6	37.7	154
180119‖	12:25:07.7476(2)	402.7(7)	110(3)	03:29.3(5)	−12:44(8)	199.5	−50.4	2.7(5)	15.9	35.5	125
180128.0	01:00:15.6179(1)	441.4(2)	51(2)	13:56(1)	−06:43(20)	326.7	52.2	2.9(3)	12.4	21.6	102
180128.2	04:54:03.7962(1)	495.9(7)	66(4)	22:22(2)	−60:15(11)	327.8	−48.6	2.3(2)	9.6	11.3	62
180130‖	04:56:06.9932(1)	343.5(4)	95(3)	21:52.2(9)	−38:34(10)	5.9	−51.8	4.1(1.0)	10.3	37.7	120
180131	05:45:42.3207(2)	657.7(5)	100(3)	21:49.9(8)	−40:41(8)	0.6	−50.7	4.5(4)	13.8	31.6	103
180212	23:45:41.39991(9)	167.5(5)	96(8)	14:21(2)	−03:35(30)	338.3	50.0	1.81(6)	18.3	21.9	79

Uncertainties are listed in parentheses. Dec., declination; DM, dispersion measure; g_l, Galactic longitude of beam centre; g_b, Galactic latitude of beam centre; R.A., right ascension; T_{obs}, total observation time on-field; $T_{\pm 15}$, time on-field within ± 15 days of FRB; w, burst full width at half maximum intensity.
*Burst arrival time referenced to a frequency of 1,297.5 MHz relative to the TAI time standard.
†Position uncertainties are 90% confidence limits and referred to the epoch J2000. Posterior localization regions are reproduced in the Supplementary Figures and are available as supplementary files, as noted in the Data availability statement.
‡S/N is the signal-to noise ratio reported in the primary beam by the search algorithm.
¶Quoted errors on fluence for FRB 171020 represent a 90% confidence limit.
‖Pulse widths are reported after deconvolution of exponential pulse broadening function (see Supplementary Information, section 1).

(1σ uncertainty). This is a factor of 200 less than the rate obtained from high Galactic latitude searches with the 64-metre Parkes radio telescope[5]. This difference is a consequence of several factors, including the burst fluence and width distributions, telescope sensitivities, and instrumental selection effects.

All bursts in the sample show strong spectral modulation, as seen in Fig. 1. While some, such as FRB 170712, show broad-band structure that persists across half of the band, many exhibit power concentrated in narrower structures of a few megahertz bandwidth, with signals absent in large fractions of the band. Others, such as FRB 170906, show strong narrow-band features imposed on broad-band structures. It is unclear whether the spectral modulation is intrinsic to the source, caused by diffractive scintillation, or a consequence of refractive propagation effects such as caustic-induced magnification[15]. The Parkes population[5]—comprising 26 bursts detected in the same frequency band as ASKAP—shows less evidence for strong spectral modulation, even at high Galactic latitudes, where Galactic propagation would be expected to impart similar spectral structure to the ASKAP bursts. There are notable counterexamples in the Parkes sample that do show spectral modulation: the highest signal-to-noise ratio Parkes detection FRB 180309 (ref. [16]); and FRB 150807, which shows spectral modulation on two scales[17]. Studies of the bright population in a different frequency range would distinguish between causes for the spectral modulation, because propagation effects are strongly frequency dependent. We averaged the spectra to estimate the global properties of the detections, finding the spectral index of combined spectra of all the bursts to be steep, with $\beta = -1.8 \pm 0.3$ over our observing band (where fluence, E, scales proportionally to frequency ν as $E(\nu) \propto \nu^{\beta}$) (see Supplementary Information, section 2).

Temporal analyses of the burst profiles are limited by the 1.26-ms time resolution of our present datasets. All of the bursts are marginally resolved beyond instrumental dispersion smearing, with a median burst full width at half maximum being 3.0 ms. This is comparable to the median burst width of the Parkes sample[18]. Three bursts (FRBs 180110, 180119 and 180130) show exponential profiles consistent with scatter broadening. The broadening time for FRB 180110 varies with frequency, scaling proportionally to $\nu^{-3.5 \pm 0.6}$, consistent with propagation through turbulent plasma[19]. FRBs 180119 and 180130 are too weak to allow us to conclusively detect a change in pulse broadening with frequency. All three also show spectral modulation; if this is caused by scattering, the presence of both pulse broadening and spectral modulation indicates that there is propagation through two distinct scattering regions along the line of sight[20,21].

As the survey frequently revisits the same positions, we can place strong constraints on burst repetition. We find no events at similar dispersion measures exceeding a signal-to-noise ratio of 9 at the dispersion measure and the positions of the ASKAP FRBs. Dwell times at these positions range from 8 days to 47 days (see Table 1), and there were 236–1,235 visits to the fields. In total, 12,456 hours of observations were conducted in the direction of the detected FRBs, and 61 days of observation of the FRB fields were conducted within ± 15 days of the FRB detection. For one of the detected bursts, FRB 171019, we conducted follow-up observations with the Parkes radio telescope two and three days after the FRB detection. In a total of 1 hour of observing, no pulses were detected at the dispersion measure of FRB 171019 above a limiting fluence of 1.5 Jy ms, which is a factor of 150 fainter than the FRB 171019 detection.

The fluence distribution of the ASKAP sample may be indicative of a cosmologically evolving population. We examined the distribution of the ASKAP sample with the V/V_{max} test statistic[22], which uses the measured signal-to-noise ratio (S/N) for each burst to assess the volume within which each burst was detected, relative to the maximum volume in which it could have been detected in Euclidean space-time. In such a population—distributed homogeneously over a volume small enough that the curvature of the Universe is negligible—the ensemble-averaged value of the statistic V/V_{max} would be 0.5. For the bursts in the

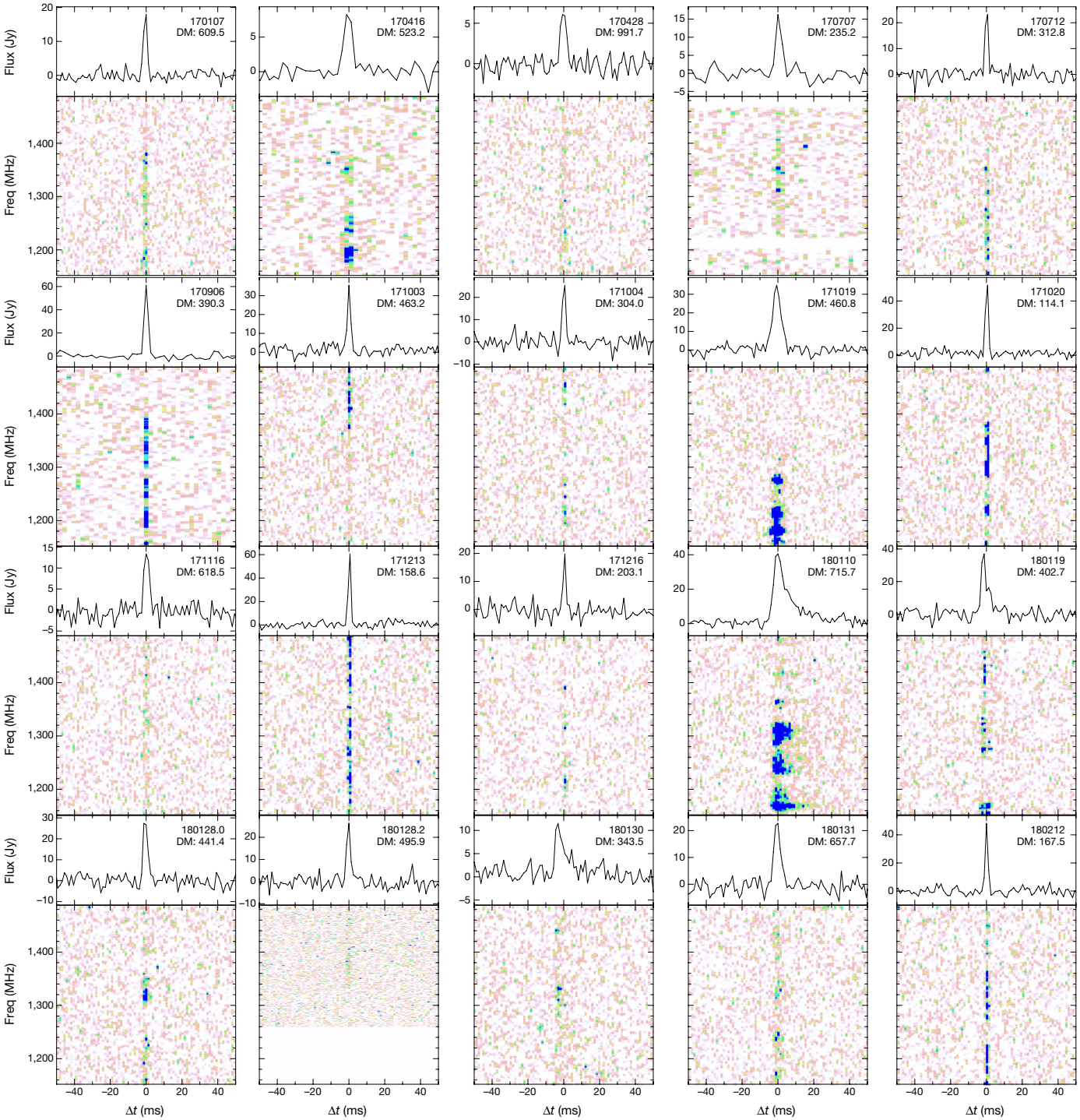

Fig. 1 | Pulse profiles and dynamic spectra of ASKAP FRBs. In the upper part of each panel the FRB name and dispersion measure (DM, in units of pc cm^{-3}) are shown, as well as the pulse profile. The lower part of each panel shows the FRB spectra, which have been dedispersed to the maximum-likelihood dispersion measure. The colour scale is set to range from the mean to 4σ of the off-pulse intensity.

ASKAP sample above our completeness threshold, we find $\langle V / V_{\rm max}\rangle = 0.58 \pm 0.07$. This is consistent with being produced by a Euclidean population with 12% confidence (see Supplementary Information, section 3). The one-sided probability was determined by simulations that model a realistic burst population with dispersion and widths consistent with the observed ASKAP population, detected by a system with our characteristics. For a pure power-law integral source count distribution, $N(>E) \propto E^{\alpha}$, parametrized by a spectral index α, the measured $V/V_{\rm max}$ value implies $\alpha = -2.1^{+0.6}_{-0.5}$ (67% confidence) over the range of fluences probed by ASKAP, evidence for steeper-than-Euclidean fluence distribution[23].

Comparison of the dispersion-measure distributions of the ASKAP and Parkes samples shows that dispersion measure is a distance indicator. The median dispersion measure of the ASKAP sample is 441 pc cm^{-3}, which is a factor of two smaller than that of the Parkes sample, 880 pc cm^{-3}. A Kolmogorov–Smirnov test finds that the probability that the two distributions are inconsistent is 99.9%. The difference in dispersion-measure distributions cannot be explained by the poorer time and frequency resolution of the ASKAP system (see Supplementary Information, section 5). This confirms both that there is both a correlation between dispersion measure and source fluence, and that dispersion measure can be used as a proxy for distance. However,

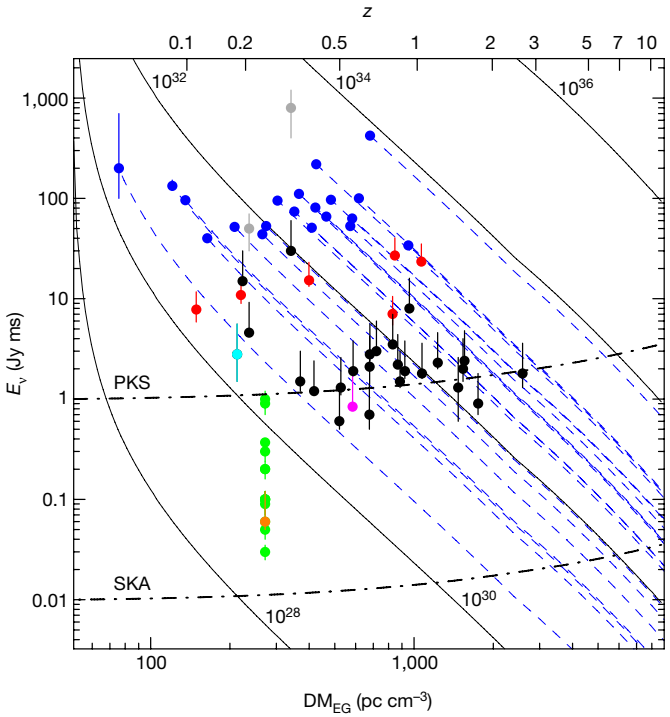

Fig. 2 | Distribution of FRB fluences and extragalactic dispersion measures. The extragalactic dispersion measures, DM_{EG}, are corrected for the inferred contribution of the Milky Way. The coloured circles denote FRBs detected with the ASKAP (blue), Parkes (black), UTMOST (red), Green Bank Telescope (magenta) and Arecibo (orange) radio telescopes. We also highlight the Parkes FRB candidate 010621 (cyan), which may be a Galactic source. Beam-corrected fluences have been estimated for two Parkes FRBs[18] (150807 and 010724) and are plotted in grey. Repeated pulses[29] from FRB 121102 are displayed in green. Uncertainties in beam fluence differ by telescope. For ASKAP and bursts from the repeating FRB 121102, we show 1σ (67% confidence) upper and lower limits. For other nonrepeating FRBs, lower limits are 1σ, but upper limits are twice the detected fluence, to reflect uncertainty in burst position within antenna pattern. The upper horizontal axis shows redshifts, assuming a homogenously distributed intergalactic plasma[10] and a host contribution of $50(1+z)^{-1}$ pc cm^{-3}, as discussed in the main text. The blue dashed curves show the fluences expected for the ASKAP-detected bursts if they were detected at larger distances (see Supplementary Information, section 4). The black curves show contours of constant spectral-energy density, in units of erg Hz^{-1}. The dash-dotted curves are lines of constant fluence, after accounting for redshift-dependent time dilation, denoting 10σ sensitivities of the Parkes radio telescope and the mid-frequency first-phase component of the future Square Kilometre Array[30] to 1-ms bursts. Further details of the data used can be found in Supplementary Information, section 4.

the difference in the distributions is smaller than would be expected for a non-evolving Euclidean population. For any individual burst, the average fluence decreases with the inverse square of distance. Because the Parkes sample is a factor of approximately 50 more sensitive than the ASKAP sample, it would be sensitive to the same source that is a factor of roughly 7 more distant. As we are comparing the median of the populations detected with Parkes and ASKAP, and not individual sources or standard candles, the ratio of dispersion measures is smaller—a consequence of a broad luminosity function for the population[24].

Figure 2 shows both the distribution of fluence plotted against extragalactic dispersion measures for all published FRBs, and the fluence/distance relationship—the latter assuming the model for host dispersion-measure contribution and extragalactic dispersion described above. The solid black curves are contours of constant energy density, calculated assuming pulses are isotropically beamed, and using the global spectral index to correct to the rest frame of the emitter. The dashed blue lines show the extrapolation of ASKAP FRB fluences to higher distances. Notably, the highest dispersion-measure event from Parkes[25]—FRB 160102—has an inferred energy comparable to those observed in ASKAP. On the basis of this extrapolation, the energies of the Parkes bursts overlap those of our sample, and are therefore more distant versions of the ASKAP events. The absence of sources above a spectral energy density of approximately 10^{34} erg Hz^{-1} for both the Parkes and the ASKAP samples is unlikely to be solely due to the frequency and temporal resolution of the data-recording systems, so could represent either a dwindling population or an energy cut-off (see Supplementary Information, section 5).

There are also marked differences between the ASKAP and Parkes burst populations, and the repeating FRB 121102. First, the ASKAP and Parkes samples show no evidence of repetition, despite large amounts of follow-up time and dense searches around the times of FRB detections. The repetition rate of FRB 121102 is intermittent, with frequent detections on month-long time scales, followed by similar length periods of apparent quiescence[3,26]. The absence of repetition enables us to reject, at the 99% confidence level, the hypothesis that all ASKAP FRBs repeat with the same properties[26] as FRB 121102 (see Supplementary Information, section 6). Second, the population of ASKAP bursts has a steep spectrum. While pulses from the repeating FRB show strong spectral modulation, equally energetic pulses are detected over a frequency range extending from 1.4 GHz to 8 GHz (ref. [27]). Furthermore, FRB 121102 is underluminous relative to the remaining bursts, as displayed in Fig. 2.

The results presented here build on previously noted differences between the repeating and the remaining non-repeating sources. For example, measurements of Faraday rotation suggest that luminous bursts propagate through dispersing plasma that is nonmagnetized[17], weakly magnetized[20,28], or has highly disordered magnetic fields. Such large Faraday rotations could still be hidden in the unpolarized FRBs, but it would be impossible to hide in the case of those with substantial polarization. By contrast, the repeating FRB source is found to have Faraday rotation (and hence magnetic-field strengths) more than four orders of magnitude larger[27]. We do not at present have the capability to measure Faraday rotation with ASKAP in FRB-search mode, but expect to upgrade these systems to make the necessary polarimetric observations shortly. We are also commissioning interferometric modes and expect to soon be able to localize detections to arcsecond accuracy. Unique identification of host galaxies will further distinguish between repeating and nonrepeating burst sources.

Code availability

The code used to conduct the FRB searches, FREDDA, will be publicly released shortly, but a pre-release version is available from K.W.B. (keith.bannister@csiro.au). Detections were processed using the dspsr (http://dspsr.sourceforge.net) and psrchive (http://psrchive.sourceforge.net) software packages for analysing pulsar and FRB data.

Data availability

Raw data files (totalling 1 PB) are archived on tape at the Pawsey Superconducting Centre. Cut-outs of the raw data, in pulsar filterbank format (http://sigproc.sourceforge.net), and posterior localization regions, are available on the CSIRO data access portal through https://doi.org/10.25919/5b6ae6b515850. Other data products are available on request from R.M.S.

Received: 8 April 2018; Accepted: 3 August 2018;
Published online: 10 October 2018

1. Lorimer, D. R., Bailes, M., McLaughlin, M. A., Narkevic, D. J. & Crawford, F. A bright millisecond radio burst of extragalactic origin. *Science* **318**, 777–780 (2007).
2. Petroff, E. et al. FRBCAT: the fast radio burst catalogue. *Publ. Astron. Soc. Aust.* **33**, e045 (2016).
3. Spitler, L. G. et al. A repeating fast radio burst. *Nature* **531**, 202–205 (2016).
4. Chatterjee, S. et al. A direct localization of a fast radio burst and its host. *Nature* **541**, 58–61 (2017).
5. Champion, D. J. et al. Five new fast radio bursts from the HTRU high-latitude survey at Parkes: first evidence for two-component bursts. *Mon. Not. R. Astron. Soc.* **460**, L30–L34 (2016).

6. McConnell, D. et al. The Australian Square Kilometre Array Pathfinder: performance of the Boolardy engineering test array. *Publ. Astron. Soc. Aust.* **33**, e042 (2016).
7. Bannister, K. W. et al. The cetection of an extremely bright fast radio burst in a phased array feed survey. *Astrophys. J.* **841**, L12 (2017).
8. Macquart, J.-P. & Johnston, S. On the paucity of fast radio bursts at low Galactic latitudes. *Mon. Not. R. Astron. Soc.* **451**, 3278–3286 (2015).
9. Xu, J. & Han, J. L. Extragalactic dispersion measures of fast radio bursts. *Res. Astron. Astrophys.* **15**, 1629 (2015).
10. Inoue, S. Probing the cosmic reionization history and local environment of gamma-ray bursts through radio dispersion. *Mon. Not. R. Astron. Soc.* **348**, 999–1008 (2004).
11. McQuinn, M. Locating the "missing" baryons with extragalactic dispersion measure estimates. *Astrophys. J.* **780**, L33 (2014).
12. Yao, J. M., Manchester, R. N. & Wang, N. A new electron-density model for estimation of pulsar and FRB distances. *Astrophys. J.* **835**, 29 (2017).
13. Meyer, M. J. et al. The HIPASS catalogue—I. Data presentation. *Mon. Not. R. Astron. Soc.* **350**, 1195–1209 (2004).
14. Jones, D. H. et al. The 6dF galaxy survey: final redshift release (DR3) and southern large-scale structures. *Mon. Not. R. Astron. Soc.* **399**, 683–698 (2009).
15. Cordes, J. M. et al. Lensing of fast radio bursts by plasma structures in host galaxies. *Astrophys. J.* **842**, 35 (2017).
16. Oslowski, S. et al. Real-time detection of an extremely high signal-to-noise ratio fast radio burst during observations of PSR J2124–3358. *Astron. Telegr.* 11385 (2018).
17. Ravi, V. et al. The magnetic field and turbulence of the cosmic web measured using a brilliant fast radio burst. *Science* **354**, 1249–1252 (2016).
18. Ravi, V. The observed properties of fast radio bursts. *Mon. Not. R. Astron. Soc.* (in the press); preprint at https://arxiv.org/abs/1710.08026 (2017).
19. Lambert, H. C. & Rickett, B. J. On the theory of pulse propagation and two-frequency field statistics in irregular interstellar plasmas. *Astrophys. J.* **517**, 299–317 (1999).
20. Masui, K. et al. Dense magnetized plasma associated with a fast radio burst. *Nature* **528**, 523–525 (2015).
21. Farah, W. et al. FRB microstructure revealed by the real-time detection of FRB170827. *Mon. Not. R. Astron. Soc.* (in the press); preprint at https://arxiv.org/abs/1803.05697 (2018).
22. Oppermann, N., Connor, L. D. & Pen, U.-L. The Euclidean distribution of fast radio bursts. *Mon. Not. R. Astron. Soc.* **461**, 984–987 (2016).
23. Macquart, J.-P. & Ekers, R. D. Fast radio burst event rate counts—I. Interpreting the observations. *Mon. Not. R. Astron. Soc.* **474**, 1900–1908 (2018).
24. von Hoerner, S. Radio source counts and cosmology. *Astrophys. J.* **186**, 741–766 (1973).
25. Bhandari, S. et al. The SUrvey for pulsars and extragalactic radio bursts—II. New FRB discoveries and their follow-up. *Mon. Not. R. Astron. Soc.* **475**, 1427–1446 (2018).
26. Law, C. J. et al. A multi-telescope campaign on FRB 121102: implications for the FRB Population. *Astrophys. J.* **850**, 76 (2017).
27. Michilli, D. et al. An extreme magneto-ionic environment associated with the fast radio burst source FRB 121102. *Nature* **553**, 182–185 (2018).
28. Keane, E. F. et al. The host galaxy of a fast radio burst. *Nature* **530**, 453–456 (2016).
29. Scholz, P. et al. The repeating fast radio burst FRB 121102: multi-wavelength observations and additional bursts. *Astrophys. J.* **833**, 177 (2016).
30. Macquart, J. P. et al. Fast transients at cosmological distances with the SKA. *Adv. Astrophys. Square Kilometre Array (AASKA14) Proc. Sci.* **215**, 55 (2015).

Acknowledgements We thank the Australia Telescope National Facility (ATNF) engineering and technical staff for their help in supporting these observations, and especially thank the staff of the Murchison Radio-astronomy observatory. We thank C. Flynn, P. Edwards, N. Tejos and V. McIntyre for comments on the manuscript, and members of the Commensal Real-time ASKAP Fast Transients (CRAFT) team for discussions. We thank the Murchison Widefield Array (MWA) principal engineer, R. Wayth, for access to the Galaxy supercomputer graphics processing units (GPU) cluster. R.M.S. and S.O. acknowledge Australian Research Council (ARC) grant FL150100148. R.M.S. also acknowledges support through ARC grant CE170100004. G.G. acknowledges support through a Commonwealth Scientific and Industrial Research Organisation (CSIRO) Office of the Chief Executive (OCE) postdoctoral fellowship. Parts of this research were conducted by the ARC Centre of Excellence for All-Sky Astrophysics (CAASTRO; grant CE110001020). This research was also supported by the ARC through grant DP18010085. The Australian SKA Pathfinder and Parkes radio telescopes are part of the ATNF, which is managed by the CSIRO. Operation of ASKAP is funded by the Australian Government with support from the National Collaborative Research Infrastructure Strategy. ASKAP uses the resources of the Pawsey Supercomputing Centre. Establishment of ASKAP, the Murchison Radio-astronomy Observatory and the Pawsey Supercomputing Centre are initiatives of the Australian Government, with support from the Government of Western Australia and the Science and Industry Endowment Fund. We acknowledge the Wajarri Yamatji people as the traditional owners of the Observatory site. This research has made use of the National Aeronautics and Space Administration (NASA)/Infrared Processing and Analysis Center (IPAC) Extragalactic Database (NED), which is operated by the Jet Propulsion Laboratory, California Institute of Technology, under contract with NASA.

Reviewer information *Nature* thanks J. Cordes, D. Lorimer and S. Ransom for their contribution to the peer review of this work.

Author contributions K.W.B. led the development of the CRAFT data-acquisition system. R.M.S., J.-P.M. and K.W.B. designed the survey. R.M.S., J-.P.M., K.W.B. and R.D.E drafted the manuscript. R.M.S. and K.W.B. conducted the observations, with assistance from A.W.H. and M.A.V. K.W.B. designed the search code. K.W.B., C.W.J., S.O., H.Q. and M.S. verified survey efficiency. R.M.S., with discussions with J.R.A., implemented the FRB localization algorithm. R.M.S., J.-P.M. and R.D.E interpreted the fluence and dispersion-measure distributions of the population. C.W.J., S.O. and J.-P.M. interpreted the nonrepetition of the ASKAP sample and compared it with the repeating FRB. R.M.S. and S.O. led searches for follow-up bursts at Parkes. E.M.S. studied the optical fields surrounding the detected FRBs. R.J.B., M.B., A.J.B., J.D.B., A.P.C., C.H., A.W.H., M.L., M.M., D.M., M.A.P, E.R.T., J.T., M.A.V. and M.T.W. contributed to development and commissioning of the CRAFT observing mode. J.R.A., C.S.A., M.E.B., J.D.C., G.G., G.H. and C.J.R. contributed to ASKAP commissioning and early science.

Competing interests The authors declare no competing interests.

Additional information

Supplementary information is available for this paper at https://doi.org/10.1038/s41586-018-0588-y.

Correspondence and requests for materials should be addressed to R.M.S. or J.-P.M.